Human Facial Soft Tissue Modeling Using Finite Element Method

Article *in* The Dhaka University studies. Part B · July 2007

CITATIONS
0

READS
3,318

3 authors:

Syukriah Kadir
Institut Teknologi Brunei
4 PUBLICATIONS **6** CITATIONS
SEE PROFILE

Tazrian Khan
University of Dhaka
2 PUBLICATIONS **5** CITATIONS
SEE PROFILE

Md. Haider Ali
University of Dhaka
49 PUBLICATIONS **323** CITATIONS
SEE PROFILE

Human Facial Soft Tissue Modeling Using Finite Element Method

S. M. Ashraful Kadir, Tazrian Khan and Md. Haider Ali

Dept. of Computer Science & Engendering,

University of Dhaka, Dhaka – 1000, Bangladesh

Email: haider@univdhaka.edu

Abstract

Finite Element Methods (FEM) procedure is an important and frequently indispensable part of engineering analysis and design. FEM computer programs are now widely used in practically all branches of engineering for the analysis of structures, solids, and fluids. In this paper we propose a FEM model of facial soft-tissue. Our ultimate target is to make a complete FEM model of human face and simulate it to create realistic facial animation. This paper discusses the finite element approach for volumetric soft-tissue modeling in the context of human-tissue simulation. Using FEM we achieve a better precision in comparison to particle systems. The shape of the presented model is taken from Computed Tomographic (CT) images using Marching Cubes (MC) algorithm. The assumed volume occupied by the soft-tissue is from the skin to the underlying bone structure. The bone structure also obtained from CT using MC with different threshold value. Experimental results obtained from a synthetic block of soft-tissue and from the Visible Human data set illustrate the performance of the envisioned model. Solid-tetrahedrons are used as the unit of the 3D volume. The use of tetrahedral FEM does not put any restriction on the geometry of the simulated volumes. The human body, especially facial soft-tissue, can be imagined as a collection of finite number of tetrahedrons. Each of the tetrahedrons has the same elastic property as the facial soft-tissue. It is potential to model the human tissue with the tetrahedrons as the building blocks. The volumetric data of the shape of human face is preserved by adaptive and multiresolution 3D finite element (tetrahedral) meshes. Experimentally we have simulated a piece of model meat (soft-tissue) attached with underlying bone by deforming it according to some external applied forces. Experiment shows that the simulated deformation is close to the reality.

Keywords

FEM, facial soft-tissue modeling, computed tomography, marching cubes algorithm, multiresolution, and soft-tissue deformation.

1. Introduction

Finite element procedures, at present, are very widely used in engineering analysis. The procedures are employed extensively in the analysis of solids and structures and of heat transfer and fluids, and indeed, Finite Element Methods (FEM's) are important and frequently indispensable part in virtually every field of engineering analysis. The development of FEM's for the solution of practical engineering problems began with the advent of digital computer[1]. And realistic modeling using FEM in Computer Graphics is gaining interest day by day.

During the past ten years, there has been growing interest in the medical and computer science field, around the simulation of medical procedures. Under the terminology proposed by Satava[2,3], the first generation of medical simulators applied the concept of navigation and immersion to 3D anatomical datasets. Those techniques, borrowed from Virtual Reality, only considered the geometrical nature of the human body. Despite their limited user interaction, those simulators found many interesting applications in the field of education or training[2]. Representing physical phenomena and, more specifically the realistic modeling of soft tissue will not only improve current medical simulation systems but will considerably enlarge the set of applications and the credibility of medical simulation, from neurosurgery planning to laparoscopic surgery simulation. In order to achieve realistic tissue deformation, it is necessary to combine deformation accuracy with computer efficiency. On the one hand, biomechanics has studied complex mathematical models and produced a large amount of experimental data for representing the deformation of soft tissue. On the other hand, computer graphics has proposed many algorithms for the real-time computation of deformable bodies,

often at the cost of ignoring the physics principles[2]. For accurate and efficient FEM calculations, it is important to have accurate and high quality models, minimize the number of elements and preserve features[4].

Our ultimate target is to simulate realistic modeling of human facial soft tissue using FEM. This paper discusses the finite element approach for volumetric soft-tissue modeling in the context of human-tissue simulation. We take the advantage of both medical data for the simulation and the consideration of facial-anatomy during the definition of muscle groups. Using FEM we achieve a better precision in comparison to particle systems. The shape of the presented model is taken from Computed Tomographic (CT) images using Marching Cubes (MC) algorithm. The assumed volume occupied by the soft-tissue is from the skin to the underlying bone structure. The bone structure also obtained from CT using MC with different threshold value. Experimental results obtained from a synthetic block of soft-tissue and from the Visible Human data set illustrate the performance of the envisioned model. We use solid-tetrahedrons as the unit of the 3D volume. The use of tetrahedral FEM does not put any restriction on the geometry of the simulated volumes. The human body, especially facial soft-tissue, can be imagined as a collection of finite number of tetrahedrons. Each of the tetrahedrons has the same elastic property as the facial soft-tissue. It is potential to model the human tissue with the tetrahedrons as the building blocks. The volumetric data of the shape of human face is preserved by adaptive and multiresolution 3D finite element (tetrahedral) meshes. In this paper, we have experimentally simulated soft-tissue deformation of a piece of meat by applying external force.

1.1 Related Works

In the last two decades the techniques of 3D modeling have developed rapidly.

1.1.2 Progressive Multiresolution Isosurface Extraction

The predominant algorithm for isosurface extraction from volume data is MC[5], which computes a local triangulation within each cube to approximate the isosurface by using a case table of edge intersections. Furthermore, the asymptotic decider[6] was proposed to avoid ambiguities existing in MC. For efficient isosurface extraction[4], starts from seed cells and traces the rest of the isosurface components by contour propagation.

To keep the face compatibility, the gravity center of the coarser triangle is inserted, and a fan of triangles is used to approximate the isosurface[7]. The chain-gang algorithm[8] was presented for isosurface rendering of super adaptive resolution (SAR) and resolves discontinuities in SAR data sets. Progressive multiresolution representation and recursive subdivision are combined effectively, and isosurfaces are constructed and smoothed by applying the edge bisection method[4]. A surface wave-front propagation technique[9] is used to generate multiresolution meshes with good aspect ratio. By combining Surface Nets[10] and the extended Marching Cubes algorithm[11], octree based Dual Contouring[12] can generate adaptive multiresolution isosurfaces with good aspect ratio and preserve sharp features[4].

1.1.3 Quality and Feature Preserving Isosurface

The enhanced distance field representation and the extended MC algorithm[13] were introduced to extract feature sensitive isosurfaces from volume data. In order to improve the representation of the surface inside each cell, a trilinear function is used to modify the MC algorithm by identifying a small number of key points inside the cell that are critical to the surface definition[14].

Elements in the extracted mesh often have bad aspect ratio. These elements then cannot be used for finite element calculations. The grid snapping method reduces the number of elements in an approximated isocontour and also improves the aspect ratio of the elements[15,16] studied how to generate triangular meshes with bounded aspect ratios from a planar point set[17] proposed an algorithm, called QMG, to triangulate a *d*-dimensional region with a bounded aspect ratio[18].

1.1.4 Quality Tetrahedral Mesh

MC is extended to extract tetrahedral meshes between two isosurfaces directly from volume data, and a Branch-on-Need Octree is used as an auxiliary data structure to accelerate the extraction process[19]. A different and systematic algorithm, Marching Tetrahedra (MT), was proposed for interval volume tetrahedralization[14]. A multiresolution framework[19] was generated by combining recursive subdivision and edge-bisection methods. Since many 3D objects are sampled in terms of slices, Bajaj et.

al introduced an approach to construct triangular surface meshes from the slice data[4]. Poor quality tetrahedra called slivers are notoriously common in 3D Delaunay triangulations. Sliver exudation[20] is used to eliminate those slivers..

1.1.5 Hexahedral Mesh Generation

Hexahedral Mesh generation is a challenging problem starts from a tetrahedral mesh to decompose each tetrahedral into four hexahedra. Although this method avoids many difficulties, it increases the number of elements[4]. Whisker Weaving[20] is an advancing front algorithm for hexahedral mesh construction, which is based on a global interpretation of the geometric dual of an all-hexahedral mesh. A trivariate subdivision scheme[4], consisting of a simple split and average algorithm, is described for hexahedral meshes.

1.1.6 Towards Realistic Soft Tissue Modeling in Medical Simulation

Herve Delingette at el. survey existing models of deformation in medical simulation and analyze the impediments to combining computer-graphics representations with biomechanical models. They noticed that most of today's medical simulation systems are based on geometric representations of anatomical structures that take no account of their physical nature[2].

1.1.7 A System for Facial Reconstruction using Distraction and Symmetry Consideration

Bugert et al. presented a system to support several facial surgeries, which are aiming to transform an unsymmetrical face to a symmetric one using two main techniques: Distraction of the lower jaw and adding or removing tissue or bone at certain facial regions. Both planning tasks are done based on segmented CT or MRI data. They used the CT-voxel information as input for the FEM. For faster calculation of soft tissue movement, they implemented a mass-spring-damper system. They also worked on consideration of soft tissue movement so the patient can see what he or she will look like after the surgery[15].

1.1.8 Anatomy-Based Facial tissue Modeling Using the Finite Element Method

Erwin et al.[21] present an anatomy-based 3D finite element tissue model. Integrated into a computer-aided surgical planning system this model allows the precise prediction of soft tissue changes resulting from the realignment of the underlying bone structure. Realistic Modeling of Elasto-Mechanical Properties of Soft Tissue and Its Evaluation

Matthias et al.[8] presented a technique, which allows comparing the simulated surgical outcome and the actual surgical result. The surgery simulation is based on a preoperative CT scan of the patient's head and on a preoperative surface scan of the patient's face. The pre- and postoperative surface scans, which are different due to the surgery, are registered employing a robust registration method, which minimizes the median of Euclidean distances of corresponding points. A mass–spring model has been developed that enables the representation of realistic nonlinear elasto-mechanical properties of multi–layer soft tissue. Global soft–tissue deformation is computed using an optimization approach.

1.1.9 Soft Tissue Modeling from 3D Scanned Data

Nebel[20] worked on 3D volumetric meshes deformation using their implementation of the FEM. They presented some experimental results of the deformation of a human body and detail a methodology to evaluate the distribution of soft tissue layers from a 3D scan of a specific individual. Their model of soft tissues consists of three elements: the epidermis, the dermis and the sub-cutis.

1.1.10 Deformation Constraints in a Mass-Spring Model to Describe Rigid Cloth Behavior

Provot presented a physically based model for animating cloth objects derived from elastically deformable models, taking the non-elastic properties of woven fabrics into account. They showed that when a concentration of high stresses occurs in a small region of the surface the local deformation becomes unrealistic compared to real deformations of textiles. The only solution to decrease these deformations has been so far to increase the stiffness of the deformed springs. They presented a new method to adapt the model to the particularly stiff properties of textiles inspired from dynamic inverse procedures[18].

1.1.11 Optimization Approaches for Soft-Tissue Prediction in Craniofacial Surgery Simulation

Matthias et al. presented a new, efficient and robust approach to soft–tissue prediction. It is based on an optimization method and has been tested with several individual patient data sets. The result of the simulation process is a 3–D, photorealistic model of the

patient's postoperative appearance that can be viewed from any position. The elasto–mechanical properties of the multi–layer soft–tissue are represented by the triangle meshes of springs[16].

1.1.12 3D Modeling of the Human Upper Limb Including the Biomecanicsof Joints, Muscles and Soft Tissues

Maurel[7] presents an investigation for the realistic modeling and animation of the upper limb in computer animation. The anatomical and biomechanical modeling of the scapulo-thoracic constraint and the shoulder joint sinus cones are proposed and applied to the realistic animation, using inverse kinematics, of a virtual skeleton and an anatomic musculoskeletal body model.

1.1.13 Physically-Based Mesh Generation: Automated Triangulation of Surfaces and Volumes via Bubble Packing

Kenji Shimada[13] proposed a physically based approach to fully automated 2D/3D triangulation that satisfies the basic requirements of element shape regularity, precise node spacing control and adaptive meshing capability. In his proposed method, mesh nodes are modeled, as bubbles with repelling/attracting forces based on proximity, much like intermolecular van der Waals forces. A static force-balancing configuration of packed bubbles is then obtained by solving the equations of motion numerically, assuming a point mass at each bubble and the effect of viscous damping.

1.2 Motivation

FEMs are well suited to compute accurate and complex deformation of soft tissue. However, it is extremely difficult to get real time performance on a moderately powerful workstation using finite element models. But for linear elastic models, only valid for small displacements, it is possible to achieve real-time deformations. Unlike spring models, there is no restriction on the stiffness value of the model with respect to the time step Δt when using semi-implicit or static schemes. The cutting or suturing operation requires the finite element model to be re-meshed.

When using structured elements such as rectangular, prismatic or hexahedral elements, the cutting is often constrained to occur along a given direction[14,19]. With unstructured elements such as triangular or tetrahedral elements, more general cut planes may be designed at the cost of greater complexity. Finally, visualization of finite elements is well suited for graphics hardware since it consists rendering visible elements. After cutting or suturing a volumetric model, it is necessary to update the list of visible facets.

2. Anatomy of Human Facial Tissue

Human skin is organized into two biaxial membranes: a relatively thin layer of stratified epithelium called the epidermis, and a thicker layer of disordered wavy coiled collagen and elastic fibers called the dermis (Figure 1)[7,17]. The elastic fibers play an important role in the skin's response at low strains: they are the first stretched when the tissue is strained whereas the collagen fibers are still crimped. They are also considerably more pliant but can be reversibly stretched to more than 100 per cent[5,7]. The epidermis and dermis are also connected by collagen fibers to a subcutaneous fatty tissue, called the *hypodermis*. This layer is sometimes considered as a third layer of skin. It appears as a honeycomb fat container structure connected to the fascia which surrounds the muscle bundles. It is the hypodermis that provides the skin's loose flexible connection with the other internal soft tissues, whereas the upper layers are more resistant to protect from injuries[5].

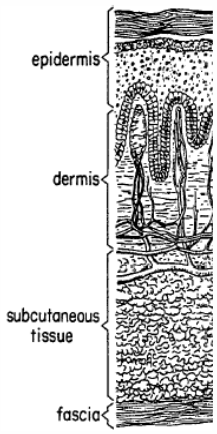

Figure 1. The skin layers[7,17]

3. Mechanical Properties Of Soft Tissue

3.1 Nonlinear Elasticity

The main property of soft tissues may be outlined as being their nonlinear elasticity. Kwan described the phenomenon as follows: "Under uniaxial tension, parallel-fibered collagenous tissues exhibit a non-

linear stress-strain relationship characterized by an initial low modulus region, an intermediate region of gradually increasing modulus, a region of maximum modulus which remains relatively constant, and a final region of decreasing modulus before complete tissue rupture occurs. The low modulus region is attributed to the removal of the undulations of collagen fibrils that normally exist in a relaxed tissue. As the fibrils start to resist the tensile load, the modulus of the tissue increases. When all the fibrils become taut and loaded, the tissue modulus reaches a maximum value, and thereafter, the tensile stress increases linearly with increasing strain.

With further loading, groups of fibrils begin to fail, causing the decrease in modulus until complete tissue rupture occurs." A typical tensile curve is shown in Figure 2. From a functional point of view, the first parts of the curve are more useful since they correspond to the physiological range in which the tissue normally functions[7,9].

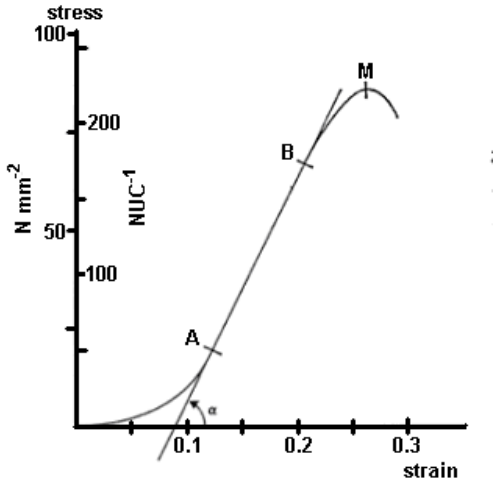

Figure 2. Load-extension Curve[7,9]

3.2 Viscoelasticity

Experimental results reveal the relationship between stress and strain in the static case. However, when the equilibrium is not reached, a history-dependent component exists in the mechanical behavior of living tissues[7,11].

When measured in dynamic extension, the stress values appear higher than those at equilibrium, for the same strain. The resulting tensile curve appears steeper than the one at equilibrium (Figure 3).

When a tissue is suddenly extended and maintained at its new length, the stress gradually decreases slowly against time. This phenomenon is called stress relaxation. When the tissue is suddenly submitted to a constant tension, its lengthening velocity decreases against time until equilibrium. This phenomenon is called creep. Under cyclic loading, the stress strain curve shows two distinct paths corresponding to the loading and unloading trajectories. This phenomenon is named hysteresis.

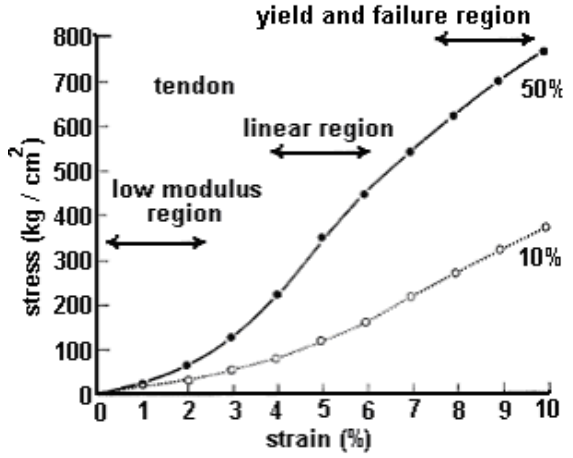

Figure 3. Influence of strain rate[7,11]

As a global statement, the stress at any instant of time depends not only on the strain at that time, but also on the history of the deformation. These mechanical properties, observed for all living tissues, are common features of a physical phenomenon named viscoelasticity[7,12].

3.3 Young's Modulus (YM)

For the description of the elastic properties of linear objects (Table 1), which are either stretched or compressed, a convenient parameter is the ration of the stress to the strain, a parameter called the YM of the material. YM can be used to predict the elongation or compression of an object as long as the stress is less the yield strength of the material.

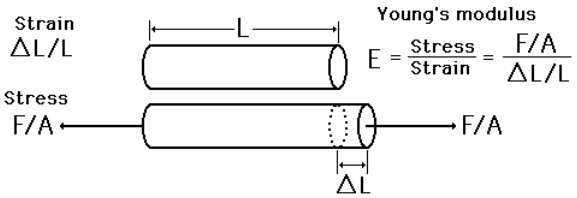

Figure 4. Young's Modulus

4. Finite Element Method

The FEM is a numerical technique that has been applied in many fields. It has become a standard tool in industry and is slowly finding its way into the field of biomechanics.

In this method, the region that is to be analyzed is discretised up into sub-regions called elements; these elements are connected at points called nodes. As we mentioned earlier, our model deals with a single types of 3D element: tetrahedrons. Once all the element stiffness matrices and force vectors have been obtained they are combined into a structure matrix equation. This equation relates nodal displacements for the entire structure to nodal loads. After applying boundary conditions the structure matrix equation can be solved to obtain unknown nodal displacements. Intra-element displacements can be interpolated from nodal values using the functions that were defined over each element[20].

Material	YM (E) in Mpa	YM (E) in PSI
Soft cuticle of pregnant locust	0.21	30
Rubber (small strain)	6.9	1000
Shell membrane of egg	7.58	1100
Human cartilage	24.13	3500
Human tendon	551.6	80,000
Unreinforced plastics, polythene, nylon	1,379	200,000
Plywood	6,895	1,000,000
Wood (along grain)	6,895	1,000,000
Fresh bone	20,685	3,000,000
Aluminum alloys	68,950	10,000,000
Iron	206,850	30,000,000
Diamond	1,172,150	170,000,000

Table 1. Approximate Young's Modulus of Various Solids[23]

5. Comparison of Soft Tissue Models

The performances of current soft tissue models are summarized in table 2. FEMs are mostly used in biomechanics, because they aim the modeling accurate deformation. On the other hand, sprint models have been developed in computer graphics for their simple and effective implementation[2].

	Deformation Accuracy	Computation Time	Cutting	Visualization
FEMs	Good	Poor	Poor	Good
Spring Models	Poor	Moderate	Moderate	Moderate
Implicit Models	Poor	Moderate	Good	Poor

Table 2. Comparison of soft tissue models

6. The Model

6.1 Basic Tetrahedral Unit for the Symmetries of a Cube

6.1.2 Symmetries of a Square

A square has 8 symmetries, 4 line reflections and 4 rotations by multiples of 90 degrees. In this figure the lines of symmetry are the two diagonal lines and the two lines connecting midpoints of opposite sides. These lines break up the square into 8 congruent isosceles right triangles. If we take one of these triangles and transform it by each of the 8 symmetries of the square, the image triangles will fill the square.

6.1.3 Planes of Symmetry of a Cube

The symmetries of a cube of side length s include two kinds of plane reflections. There are 3 symmetries that are reflections in a plane parallel to a pair of faces of the cube. Each of these 3 planes intersects 4 edges at their midpoints; it is the perpendicular bisecting plane of 4 parallel edges. The symmetry plane cuts the surface of the cube in a square of side s. Each of the planes intersects 4 square faces. It intersects each face along a line of symmetry of the face that connects midpoints of opposite edges. Such a plane contains none of the vertices of the cube.

The other 6 plane reflections are in planes that cut two opposite faces of cubes in diagonals. Such a plane contains two opposite edges of the cube and 4 vertices. Each such plane cuts the surface of the cube in a rectangle of width=s and length=s*sqrt 2.

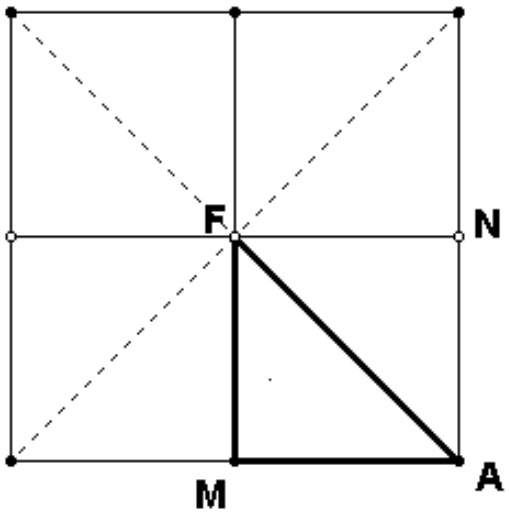

Figure 5. Symmetries of a square

In the square figure above, if the square is a face of the cube, then two of the 3 planes of symmetry of the first type cut the square along the two lines of symmetry through the midpoints of the sides. Also, two of the 6 planes of symmetry of the second type cut the square along the lines of symmetry that are diagonals of the square. Thus these planes cut each face of the cube into the same 8 congruent isosceles right triangles that were the fundamental regions of the symmetries of the square. Since there are six faces, the surface of the cube is cut into 48 congruent isosceles right triangles.

6.1.4 Fundamental Regions of the Cube

We have seen how the surface of the cube is cut into 48 right triangles by the planes of symmetry of the cube. The interior of the cube is cut into solid polyhedral pieces. Since all the planes of symmetry pass through the center O of the cube, the cube is cut into 48 pyramids with vertex O and with base on of the 48 triangles.

Each pyramid is an irregular tetrahedron. One face is one of the 48 triangles on the faces of the cube. The three other faces are triangles; each has a vertex at O. Each of these faces of the pyramid is a triangle in one of the planes of symmetry of the cube. We can see that one of these planes of symmetry is the type parallel to a pair of faces of the cube. The other two are each planes that contain a pair of edges.

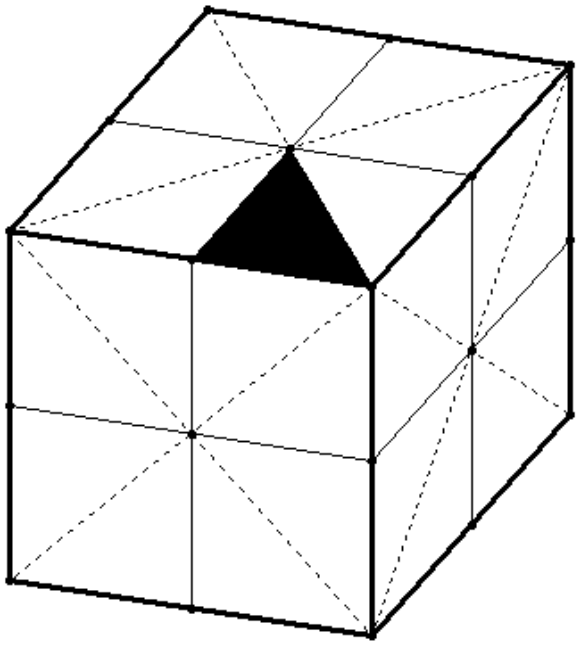

Figure 6. Symmetry of a cube

6.1.5 Measurements for the units

In the figure the vertices of one of the 48 triangles are labeled AFM.

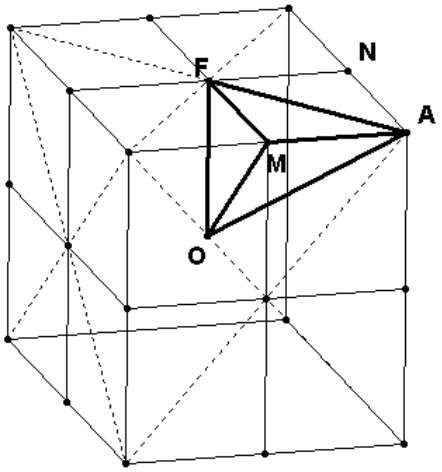

Figure 7. Fundamental regions of a cube

Then the faces of the pyramid are triangle AFM (on the face of the cube), triangle OFM (on the plane of symmetry parallel to two cube faces and perpendicular to line AM), triangle OMA (on the plane of symmetry that contains O and line AM) and triangle OAF (on the plane of symmetry that cuts a face in line AF).

If we examine the edges of the pyramid further, we see that the edge OF is perpendicular to the face AFM.

Also the lengths of 3 edges of the pyramid are equal to s/2; these are AM = MR = FO. Two edges are diagonals of squares, so AF = OM = (s/2)*sqrt 3. The final edge is one half the diameter of the cube OA = (s/2)*sqrt 3 (OA is the diagonal of a "corner cube").

Thus we see that among the four faces of the tetrahedron, there are two pairs of congruent triangles. Two are isosceles right triangles with legs = s/2 and two are right triangles that are halves of the rectangle with width s/2 and length (s/2)*sqrt 2. The parallelogram and rectangle below can be cut out and folded along the indicated diagonal and then attached to form the pyramid.

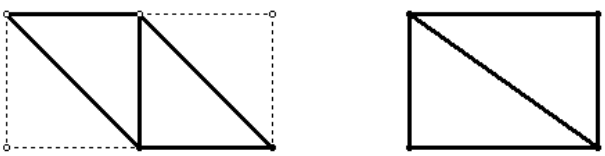

Figure 8. Folded tetrahedron

It is easy to check that the volume of one of these pyramids is 1/48 of the volume of the cube.

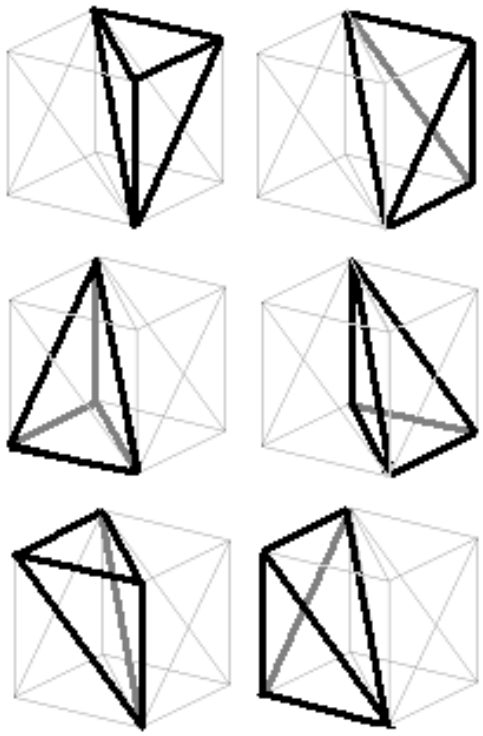

Figure 9. Unit tetrahedrons

6.2 Building the Model

6.2.2 Tetrahedral Unit

As we mentioned earlier, we use solid regular shaped tetrahedrons as the basic unit of our finite element model. These tetrahedrons preserve the finite element properties of human soft-tissue. Figure 8 illustrates the folded tetrahedrons. Figure 9 shows the structure of a cube with tetrahedrons. This is clear from the images that a tetrahedron always covers half of two planes of a cube, which are placed in 90^0 3D angles.

Four corners of each of the tetrahedrons is the voxels of the 3D mesh. Each voxel is shared by two or more tetrahedrons. A voxel can be shared by maximum 48 tetrahedrons.

Each of the 4 sides of the tetrahedrons is the edges of the tetrahedrons, and can be assumed as the fibres of human soft-tissue. Each of these edges has the exact mechanical properties of human soft-tissue. These edges are stressed with the external pressure preserving the property of human tissue. These edges may be enlarged or squeezed depending on angle of the applied force and other parameters.

The vertices of the mesh move to newer places according the changes of size of the edges. The change of the size of each edge is up to a level, which is assumed for the experiment. We assumed the maximum increase of an edge can be up to 50% of the original length and the decrease can be up to 25%. Whatever may be the magnitude of the applied force the deformation of the edges will be limited to that assumption. If the pressure exceeds the maximum tolerable stress, the edge will be broken; the result will be two disconnected vertices in respect to the edge.

6.2.3 Six Tetrahedrons build up a Unit Cube

The tetrahedrons build up a cube as a larger unit. Figure 10 shows the smallest cube for the mesh generation. Each of the smaller cubes contains 6 tetrahedrons; a corner point of the cube is connected to each other points of the cube, this point is the common point of the 6 tetrahedrons packed in the smallest cube (Figure 10).

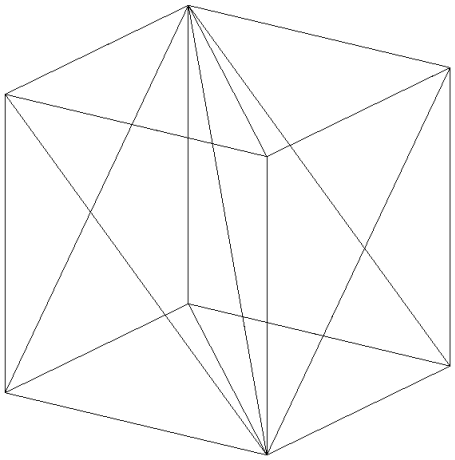

Figure 10. Smaller cubes contains 6 tetrahedrons, the nearest bottom point is connected to each other points of the cube

6.2.4 Smallest Part of the Mesh with Complete Properties

The smallest unit of the mesh that preserves all the properties of the complete mesh is a cube and contains 48 tetrahedrons packed in 8 different smaller cubes of figure 10. The smaller cubes are symmetric, but not fabricated in different direction. The common points of the 8 tetrahedrons meet in the center of the cube in Figure 11. The cube built with the 8 smallest cubes becomes more stable, and so the complete mesh.

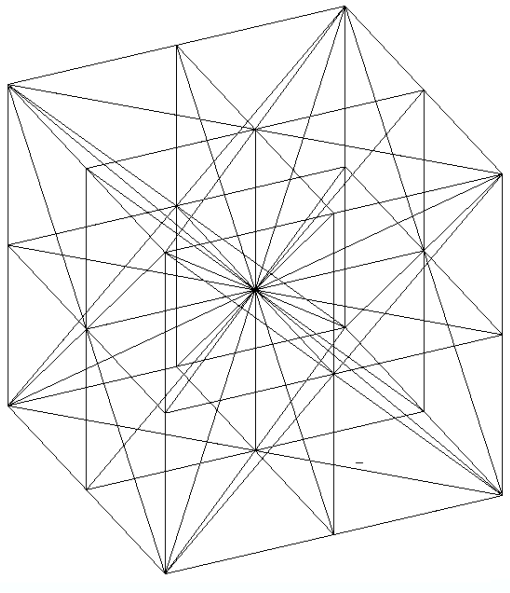

Figure 11. 3D-Meshing with tetrahedrons. 6 tetrahedrons create a cube, 8 cubes create a unit for the mesh, i.e. 48 tetrahedrons create a unit

The cube in figure 11 can be imagines in another point of view as it has a center point. Each of the 48 tetrahedrons shares the center point of the cube. Thus the force applied to any vertex transfers a part of the force to the center. As the center is connected with each of the other nodes, the force is eventually transferred to each of the nodes and edges in the cube, according to the angle. The applied force is distributed to all the tetrahedrons regularly, which makes the FEM more appropriate.

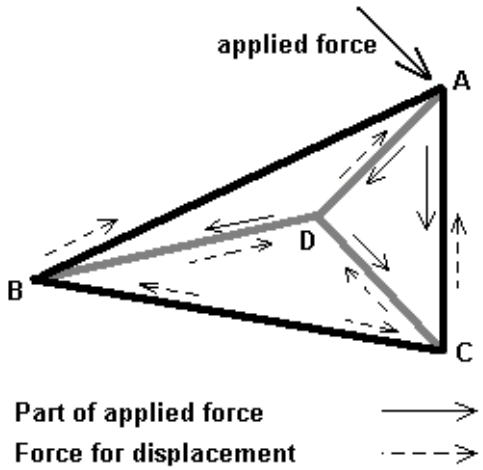

Figure 12. Distribution of applied force

6.3 Force Model

Figure 12 demonstrates the force distribution from a node of a tetrahedron to the other three nodes. In the figure the external force is applied to vertex A, which is distributed to the vertices C and D. The force is distributed with the application of 3D vector analysis.

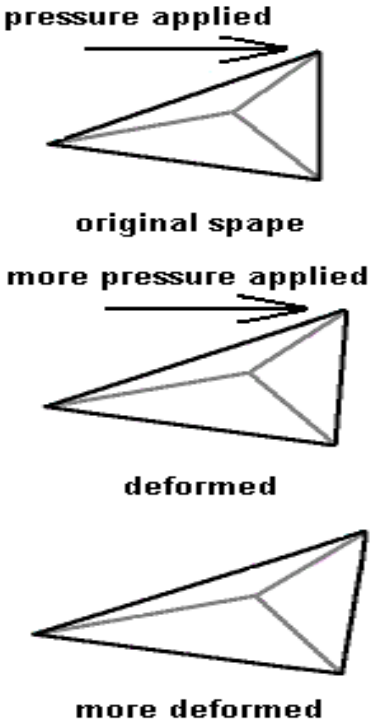

Figure 13. Deformation of a tetrahedron for external force

In the figure the angle between AB and the force is greater than 90^0, so there is no direct force from A to B.

The force is ultimately transferred to B through D while the force applied to D is through AD, which obviously transfer its part to A through DA. The figure gives an idea about the created force for the displacement of nodes, which will be applied recursively to the other nodes. The force application and deformation process can be presented in algorithm 6.3.

Algorithm 6.3 Force Applied

For each vertex of the mesh

1. Calculate displacement of vertex for force.
2. Check the displacement is applicable in current condition.
3. If the displacement is applicable store it as pending movement of the node.
4. If the displacement is not applicable, calculate and store maximum applicable displacement depending on the connected nodes and edges and distribute extra force to the appropriate nodes as applied force according to 3D vector analysis.

5. Distribute the part of the force to the connected nodes as applied force according to 3D vector analysis.
6. Apply deformation.
7. Distribute the produced force for node displacement to appropriate connecting nodes as applied force according to 3D vector analysis.

The conditions in step 2 of algorithm 6.3 are the limitations of elasticity and compressibility of each of the connected nodes. If a node-displacement tries to expand or squeeze the edge beyond the limitation, the node may cause extra force to preserve the property of maximum possible deformation. The edges near to the bone structure have less elasticity and compressibility than the edges near to the skin.

7. The Result

We have developed an interactive program for 3D mesh extraction and rendering from volumetric data sets. The interface provides the 3D tissue model, which includes element coordinates, their boundary conditions and given displacements due to bone realignment. In our first application, we assume the stress-strain relationship to be linearly elastic. As mentioned earlier human tissue is non-linearly elastic and we are currently working on a non-linear formulation to improve our model.

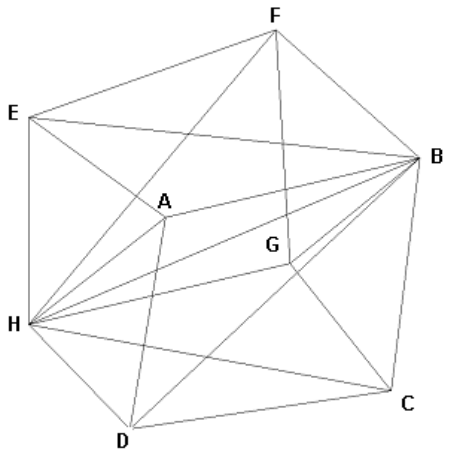

Figure 14. Deformation of a cube

Experimentally we have simulated the deformation of a piece of meat with our generated mesh. Figure 13 illustrates the deformation of a tetrahedron for the applied external force. With the increase of applied force the tetrahedron is deformed more. The tetrahedral shape is preserved as well.

In figure 14 the deformation of a cube is illustrated. The pressure is applied on node B horizontally from left to right according to the image here. It is understandable that the pressure is applied to the other nodes and node A responses to the transferred pressure the most.

Figure 15 demonstrates the deformation for force applied to the smallest cubic mesh, which contains all the properties of a large model. The pressure is applied in the left plane of the model in the figure. The point is pushed down as illustrated in the deformed image in figure 15.

Model of a piece of meat and simulated deformations are shown in figure 16 to 18.

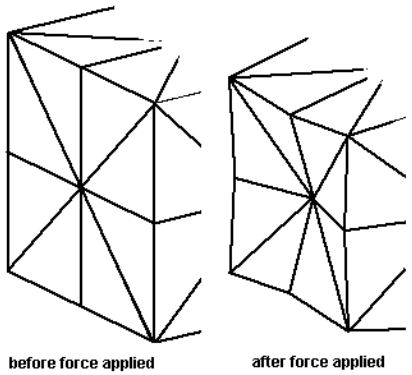

Figure 15. Deformation of the smallest complete model

8. Conclusion and Future Works

In this paper, we have presented a tetrahedral 3D finite element soft-tissue model of a piece of meat attached with underlying bone, which allows the precise prediction of tissue changes according to some external applied forces. Experimentally we have simulated the piece of model meat deformation with variation of external forces. Experiment shows that the simulated deformation is close to the reality. This is the beginning of a large goal to make a complete FEM model of human face and simulate it to create realistic facial animation. After completion of our research we will be able to implement the realistic model in various potential field of biomedical engineering, for example, simulation of facial soft tissue with the movement of underlying bone structure. We will be able to simulate the changes of human facial expressions after the surgical replacement of facial skin with the skin of the other part of human body.

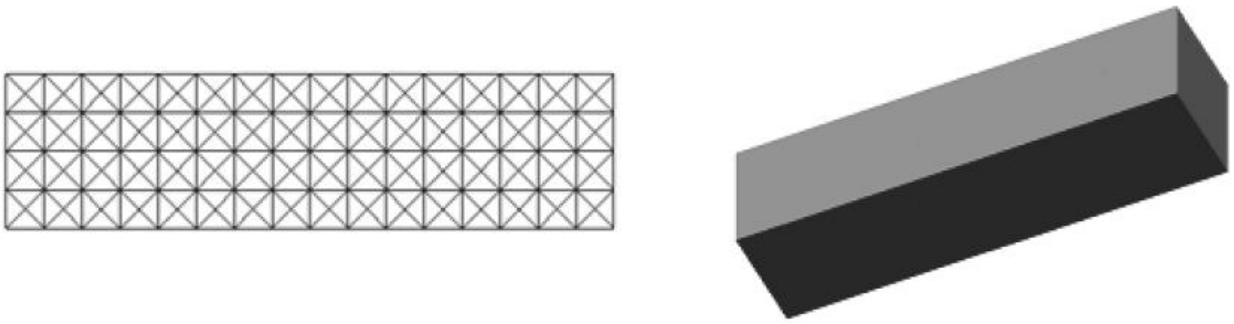

Figure 16. Model of the piece of meat (soft-tissue). The mesh at left-hand side is a side view o the mesh. This side view is useful to understand the shape changes with external applied force. The right-hand side one is the solid model of the piece of meat

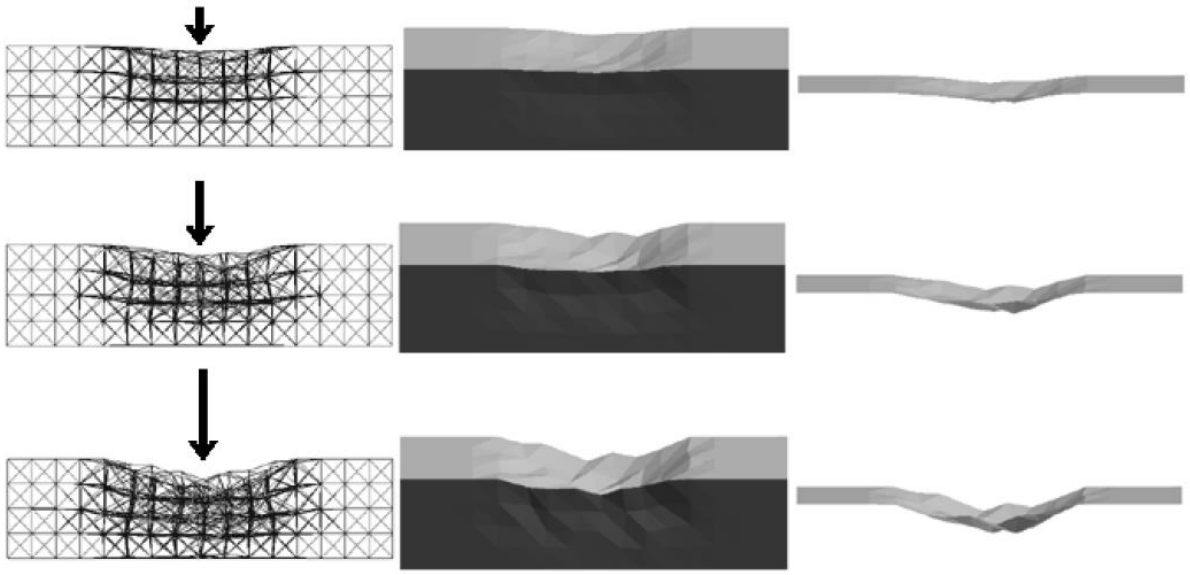

Figure 17. Deformation of the model for applied force. The arrow in the figure is the presentation of applied force. The length of the arrow is proportional to the applied force magnitude. The force is applied in the middle of the model meat model. Right hand side images in this figure represent the skin layer

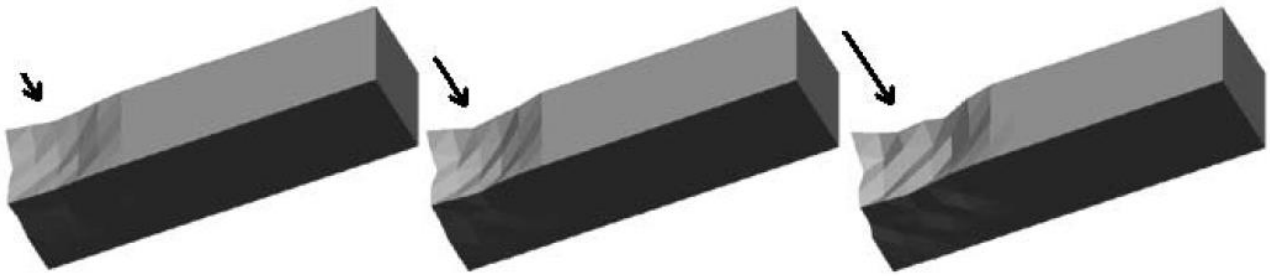

Figure 18. Deformation of the piece of solid meat model due to applied force on the side of the model. The arrows represent the applied forces. The lengths of the arrows are proportional to the magnitude of applied forces

9. References

[1] Klaus-Jürgen Bathe, *Finite Element Procedures*, Prentice-Hall, Inc., Englewood Cliffs, N.J., U.S.A. (April 2002).

[2] Herve Delingette, *Towards Realistic Soft Tissue Modeling in Medical Simulation*, Proceedings of the IEEE: Special Issue on Surgery Simulation, pp. 512-523, April (1998).

[3] R. Satava, *Medical virtual reality: The current status of the future*, In Proc. of 4th conf. Medicine Meets Virtual Reality (MMVR IV), pp. 100-106 (1996).

[4] *Yongjie* Zhang, Chandrajit Bajaj and Bong-Soo Sohn, *Adaptive Multiresolution and Quality 3D Meshing from Imaging Data*, Texas Institute for Computational and Applied Mathematics, The University of Texas at Austin, 1996.

http://www.ticam.utexas.edu/reports/2002/0242.pdf.

[5] Y. Lanir, *Skin mechanics*, Handbook of Bioengineering, by R. Skalak, S. Chien, New York, McGraw-Hill (1987).

[6] D.E. Birk, F.H. Silver, R.L. Trelstad, *Matrix assembly, in Cell Biology of Extracellular Matrix*, 2nd Edn. By E.D. Hay. New York: Plenum Press (1991)

[7] Walter Maurel, *3D Modeling of the Human Upper Limb Including the Biomechanics of Joints, Muscles and Soft Tissues*, Departement d'Informatique, Ecole Polytechnique Federale de Lausanne (Thesis no 1906 (1998)).

[8] Matthias Teschner, Sabine Girod, Bernd Girod, *Realistic Modeling of Elasto–Mechanical Properties of Soft Tissue and Its Evaluation*, National Biocomputation Center, Information Systems Laboratory, Stanford University, USA.

[9] M.K. Kwan, S L-Y. Woo, *A structural model to describe the nonlinear stress-strain behavior for parallel-fibered collagenous tissues*, J. Biomech. Engng, 111, 361–363 (1989).

[10] A. Viidik, J. Vuust, *Biology of collagen, Proceedings of a symposium*, Aarhus (July/August 1978). London: Academic Press (1980).

[11] Y.C. Fung, N. Perrone, M. Anliker. Englewood Cliffs, *Stress-strain history relations of soft tissues in simple elongation*, in Biomechanics: Its Foundations and Objectives, NJ: Prentice-Hall (1972).

[12] Y.C. Fung, *Bioviscoelastic Solids*, in Biomechanics: Mechanical Properties of Living Tissues. Berlin: Springer-Verlag (1993). (14) G. J. Song and N. P. Reddy, *Tissue Cutting In Virtual Environment, In Medecine Meets Virtual Reality* IV, pp. 359-364. IOS Press, (1995).

[13] Kenji Shimada, *Physically-Based Mesh Generation: Automated Triangulation of Surfaces and Volumes via Bubble Packing*, Thesis for the Doctor of Philosophy in Mechanical Engineering.

http://graphics.ethz.ch/~teschner/publications/evaluationCARS2001.pdf

[14] Cornelia Kober, Matthias Müller-Hannemann, *Hexahedral Mesh Generation for the Simulation of the Human Mandible*, Proceedings of the 9th International Meshing Roundtable, New Orleans, Louisiana 1998.

[15] O. Burgert, T. Salb, T. Gockel, R. Dillmann , S. Hassfeld, J. Brief, R. Krempien, S. Walz, J. Mühling, *A System for Facial Reconstruction using Distraction and Symmetry Consideration*, German Research Foundation by the SFB414, (Project Q45).

http://wwwiaim.ira.uka.de/Publications/2001/burgert-CARS2001.pdf

[16] Matthias Teschner, Sabine Girod, and Bernd Girod, *Optimization Approaches for Soft–Tissue Prediction in Craniofacial Surgery Simulation*,Second Int. Conf. on Medical Image Computing and Computer-Assisted Intervention MICCAI'99, Cambridge, England, (September 19-22, 1999).

[17] D.A. Danielson, *Human skin as an elastic membrane*, J. Biomechanics, Vol. 6, pp. 539-546 (1973).

[18] Xavier Provot, *Deformation Constraints in a Mass-Spring Model to Describe Rigid Cloth Behavior*, Institute National de Recherche en Informatique et Automatique (INRIA), France.

http://graphics.stanford.edu/courses/cs468-02winter/Papers/Rigidcloth.pdf

[19] Kaiss, M. and Le Tallec, P. *La Modelisation numerique du contact ceil-trepan*, Revue Europeenne des Elements Finis, 5(3): 375-408 (February 1996).

http://www.miralab.unige.ch/papers/60.pdf

[20] Jean-Christophe Nebel, *Soft tissue modeling from 3D scanned data*, Department of Computing Science, University of Glasgow, Glasgow, UK.

http://www.brc.dcs.gla.ac.uk/~jc/Papers/PDFformat/Geneva00.pdf

[21] *Erwin Keeve, Sabine Girod, Paula Pfeifle, and Bernd Girod, Anatomy-based facial tissue modeling using the finite element method, Proceedings of IEEE Visualization, Pages: 21-28,.1996*

[22] Wikipedia, *Approximate Young's Moduli of Various Solids*, this article is available online:

http://en.wikipedia.org/wiki/Young%27s_modulus